HHS Public Access

Author manuscript

Gene Expr Patterns. Author manuscript; available in PMC 2024 June 01.

Published in final edited form as:

Gene Expr Patterns. 2023 June ; 48: 119319. doi:10.1016/j.gep.2023.119319.

hnRNPL Expression Dynamics in the Embryo and Placenta

Vineetha Mathew[1], **Ariel Mei**[1], **Hamida Giwa**[1], **Agnes Cheong**[2], **Ashmita Chander**[2], **Aaron Zou**[3], **Robert M. Blanton**[3], **Olga Kashpur**[1], **Wei Cui**[2], **Donna Slonim**[4], **Taysir Mahmoud**[1], **Perrie O'Tierney-Ginn**[1], **Jesse Mager**[2], **Isabelle Draper**[3], **Mary C. Wallingford**[1,3]

[1]Mother Infant Research Institute, Tufts Medical Center, 800 Washington St, Boston, MA, 02111, USA.

[2]Department of Veterinary and Animal Sciences, University of Massachusetts, Amherst, MA, 01003, USA.

[3]Molecular Cardiology Research Institute, Tufts Medical Center, 800 Washington St, Boston, MA, 02111, USA.

[4]Department of Computer Science, Tufts University, 177 College Avenue, Medford, MA, 02155, USA.

Abstract

Heterogeneous nuclear ribonucleoprotein L (hnRNPL) is a conserved RNA binding protein (RBP) that plays an important role in the alternative splicing of gene transcripts, and thus in the generation of specific protein isoforms. Global deficiency in hnRNPL in mice results in preimplantation embryonic lethality at embryonic day (E) 3.5. To begin to understand the contribution of hnRNPL-regulated pathways in the normal development of the embryo and placenta, we determined hnRNPL expression profile and subcellular localization throughout development. Proteome and Western blot analyses were employed to determine hnRNPL abundance between E3.5 and E17.5. Histological analyses supported that the embryo and implantation site display distinct hnRNPL localization patterns. In the fully developed mouse placenta, nuclear hnRNPL was observed broadly in trophoblasts, whereas within the implantation site a discrete subset of cells showed hnRNPL outside the nucleus. In the first-trimester human placenta, hnRNPL was detected in the undifferentiated cytotrophoblasts, suggesting a role for this factor in trophoblast progenitors. Parallel *in vitro* studies utilizing Htr8 and Jeg3 cell lines confirmed expression of hnRNPL in cellular models of human trophoblasts. These studies coordinated regulation of hnRNPL during the normal developmental program in the mammalian embryo and placenta.

Corresponding Author Mary C. Wallingford, Mother Infant Research Institute, Tufts Medical Center, 800 Washington St., Boston, MA 02111, marycwallingford@gmail.com, Office: 1+617-636-5982, Fax: 1+617-636-1469.

Keywords

heterogeneous nuclear proteins; hnRNPL; posttranscriptional regulation; preimplantation; splicing factors; trophectoderm; trophoblasts

1. INTRODUCTION

The vast majority of mammalian genes are alternatively spliced, permitting generation of diverse protein isoforms to address changing developmental requirements and environmental exposures of specific cells and tissues. This dynamic process is controlled by members of the RNA binding protein (RBP) family. Heterogeneous nuclear ribonucleoprotein L (hnRNPL) is a conserved RBP and global splicing factor (SF) that binds consensus CA-rich regions on mRNA targets via its RNA Recognition Motifs (RRMs) (Hui et al., 2005; Hung et al., 2008). In addition to its well-established role in alternative splicing, hnRNPL also regulates mRNA nuclear export, stability and translation (Geuens et al., 2016; Guang et al., 2005; Hahm et al., 1998; Majumder et al., 2009; Shih & Claffey, 1999). Furthermore, hnRNPL has been implicated in epigenetic regulation of gene expression through regulation of SET domain containing 2, histone lysine methyltransferase (SETD2) and histone 3 lysine 36 methylation (H3K36me) (Yuan et al., 2009).

Previous studies using tissue-specific knockout mice have unraveled a critical role for hnRNPL in the maintenance, proliferation and differentiation of stem cells, in the hematopoietic lineage (Gaudreau et al., 2016), and ameloblast cell lineage (Xiao Liu et al., 2020). *In vitro* studies support an essential function of hnRNPL in maintenance of epidermal stem cell identity (J. Li et al., 2021). Work in Drosophila, zebrafish and human cell lines indicates that hnRNPL deficiency is detrimental to myogenesis/muscle development (Alexander et al., 2021; Draper et al., 2009). However, the molecular and cellular mechanisms that underlie the observed early, blastocyst stage embryonic lethality that results from overall loss of hnRNPL in mice (Gaudreau et al., 2012) remain largely unknown.

In eutherian mammals, development can be described in discrete developmental stages which are followed by growth and maturation, including: preimplantation, peri-implantation, and postimplantation development. During early preimplantation development, the fertilized zygote undergoes zygotic gene activation and significant epigenetic transitions (Alam et al., 2015; Marcho et al., 2015). Successive cell divisions produce blastomeres and the zygote progresses through the 2-cell, 4-cell, 8-cell, morula and blastocysts stages. The early blastocyst is characterized by an outer epithelial sheet of trophectoderm, an inner blastocoel cavity, and a population of cells on one side of the inner wall of the trophectoderm termed the inner cell mass (ICM) which is the source of the entirety of the fetus, as well as embryonic stem cells *in vitro*. In the mouse, peri-implantation development and placentation are initiated when the blastocyst comes in sustained contact with maternal tissue as described in detail in Wallingford et al 2013 (Wallingford et al., 2013). As postimplantation development continues, the decidua, decidual glands, and decidual vasculature are remodeled, an intricate maternal-fetal interface in the placenta as

specialized vasculature develops and uterine arteries are remodeled, and the embryo proper completes implantation and progresses through gastrulation and organogenesis.

In the current study we examined the potential coordinated regulation of hnRNPL in the developing mouse. We hypothesized that hnRNPL expression would increase at the blastocyst stage of preimplantation development and predicted a peak in protein abundance in the trophectoderm lineage. To test this hypothesis, we determined hnRNPL mRNA expression levels and protein localization dynamics in the developing mouse and in the mature mouse and human placenta.

2. RESULTS

2.1 hnRNPL is Expressed in the Early Mouse Embryo and Placenta

In order to elucidate potential roles of hnRNPL in early development, we first sought to determine the developmental stages during which hnRNPL mRNA and protein are detected. RT-PCR analysis of oocytes, extraembryonic tissues, and embryonic tissues was performed to quantify the expression levels of hnRNPL mRNA during development. Mouse oocytes and embryos between the zygote and E8.5 stages of development were examined (Figure 1A). hnRNPL mRNA was detected at all stages, including oocytes, preimplantation stages (zygote-blastocyst), peri-implantation stages (E4.5) and postimplantation embryos (E5.5–8.5) with consistent levels of mRNA expression throughout.

We then sought to analyze cell-type specific protein expression of hnRNPL. Antibody immunofluorescence (IF) was employed to characterize the localization pattern of hnRNPL protein in various cell types across development. hnRNPL protein detection in the preimplantation blastocyst stage was assessed using whole mount IF and semi-quantitative image analysis (Figure 1B–F). hnRNPL was observed in both the OCT4 positive inner cell mass (ICM), which gives rise to the epiblast and primitive endoderm cells, as well as OCT4 negative trophectoderm, which gives rise to trophoblast lineages. To test whether hnRNPL is more highly expressed in the ICM or trophectoderm, semi-quantitative image analysis was conducted using blastocysts stained with antibodies against hnRNPL and OCT4 (Figure C-F), as well as CDX2 (not shown) (N=7). The results supported that hnRNPL is detected in both cell types, but the level of hnRNPL is significantly higher (p-value=1.55319E-05) in trophectoderm cells (Figure 1B). hnRNPL and OCT4 were similarly assessed at E4.5 through immunofluorescence of paraffin embedded tissue sections. At this stage we observed a loss of hnRNPL in decidual cells at the implantation site directly adjacent to the developing embryo (dashed lines in Figure 1G and Supplemental Figure 1).

2.2 Localization of hnRNPL during Postimplantation Development

Subsequent tissue section IHC was carried out to assess hnRNPL expression in postimplantation embryos, specifically between E5.5 to E8.5 (Figure 2) Although hnRNPL was still ubiquitously expressed in cells at and surrounding the implantation site, we observed qualitative differences in several cell-types. The visceral endoderm (VE) and ectoplacental cone (EPC) showed a relatively higher signal compared to that in surrounding decidual cells (Figure 2). This pattern was consistent from E5.5 to E8.5. At E7.5 and

E8.5 stage, we observed strong hnRNPL expression in uterine natural killer (uNK) cells at the implantation site (Figure 2E–F). In contrast, fetal blood cells in the placenta at E8.5 appeared to be overall hnRNPL negative, similar to the previous observation at the E5.5 maternal decidua (arrows in Figure 1I). In embryo proper we observed that hnRNPL was highest in the fetal heart at E8.5 (Figure 2J–K). Finally, to evaluate stage-specific correlation of hnRNPL expression in the developing heart, hnRNPL transcript levels were examined (Figure 2L). hnRNPL levels were abundant in the developing heart when compared to the postnatal (P) heart. A peak was observed at E11.5 and levels consistently declined after P0. With respect to morphogenesis of the developing heart, E11.5 correlates with proliferation of the myocardium and expansion of the cardiovascular lumen in relation to the myocardium (de Boer et al., 2012) as well as the initiation of atrial and ventricular maturation (Koibuchi & Chin, 2007). To test hnRNPL expression from embryonic development to adulthood, we performed immunoblot for hnRNPL in heart tissue from embryos (day E9.5), neonatal mice (PN1), and adults 22 weeks of age (Figure 3). We observed highest hnRNPL expression, normalized to GAPDH, during the embryonic period. In the adult heart, hnRNPL expression increased compared with neonatal expression. Notably, the low molecular weight isoform of hnRNPL became more prominent in the adult heart.

Overall, hnRNPL was found to be ubiquitously expressed, with select cell types displaying very high or little to no hnRNPL expression, such as the fetal heart or fetal blood cells, respectively. Aside from the semi-quantitative observations of hnRNPL expression, we observed that trophoblast giant cells (TGC), exhibited hnRNPL expression in a predominantly peripheral distribution in the nucleus, rather than the typical, diffuse nuclear pattern seen in other cells (Figure 2D; Figure 4). We then posed the hypothesis that hnRNPL localization is skewed to the peripheral nuclear compartment, also referred to as compartment B which is associated with epigenetic regulation. Measurements of integrated density in TGC nuclear compartments revealed increased hnRNPL signal in the nuclear periphery compared to the nuclear center (p-value= 4.24888E-23) (Figure 4C).

2.3 Placental Expression of hnRNPL

We then examined hnRNPL localization in the placenta through immunofluorescence and longitudinal abundance levels of hnRNPL protein through the use of tandem mass spec. RT-PCR confirmed hnRNPL mRNA expression was present in E13.5 mouse placenta (Figure 5A). Tandem mass spectrometry data was analyzed in a proteomics analysis pipeline (Kashpur et al in process) to visualize the temporal protein abundance of hnRNPL between E8.5 and E17.5 to examine whether fluctuations in expression level associated with a particular stage of placentation (Figure 5B). Protein quantitation indicated consistent presence of this protein throughout the analyzed time-period with minimal fluctuation. A single peak in expression was observed in the E8.5 chorion, reaching nearly 20 a.u., compared to a baseline expression of ~12 a.u. in the E8.5 allantois and developing placenta. Temporal expression of the paralog protein hnRNPL-like (hnRNPLL) was also measured in this study. hnRNPLL was only minimally detected and exhibited no variation in expression during placental development. From this we concluded that all reported results were specific to the hnRNPL protein.

We next examined hnRNPL expression by immunofluorescence in the E13.5 placental labyrinth (Figure 5C) and spiral arteries (Figure 5D) of the mouse placenta. Trophoblast cells were identified by cytokeratin-7 (CK7) positivity. hnRNPL was ubiquitously expressed at E13.5 and detected in CK7 positive trophoblasts (Figure 5D).

Localization patterns of hnRNPL were further analyzed in the mature placenta and associated tissues at E17.5 (Figure 6) using CK7 as a counterstain. As expected, hnRNPL was observed in the uterine muscle (Figure 6A–D), as well as the yolk sac (Figure 6E–H), which harbors terminal visceral endoderm identified previously to express high levels of hnRNPL early in development (Figure 2). In the placenta, hnRNPL exhibited ubiquitous expression across all tissue types adjacent to trophoblast cells and across the trilaminar structure consisting of decidua, junctional zone, and labyrinth (Figure 6I–P). Trophoblast cells were CK7 positive and were visualized most prominently in the labyrinth and lining spiral arteries in the junctional zone. The junctional zone showed greater levels of hnRNPL that could be seen more distinctly compared to the lower intensity expression seen across the labyrinth (Figure 6I–L).

First trimester human placenta samples and human cell lines were obtained to evaluate hnRNPL localization in a human correlate (Figure 7). In these sections we saw hnRNPL colocalized with CK7 positive cytotrophoblast cells with minimal expression seen in the syncytiotrophoblast layers (Figure 7A–H). Expression of hnRNPL in human trophoblasts was confirmed *in vitro* through immunocytochemistry experiments using Htr8 and Jeg3 trophoblast cell lines (Figure 7I–L).

Altogether, spatiotemporally-specific hnRNPL expression patterns were observed (Table 1). These findings demonstrate the ubiquity of hnRNPL expression in embryonic and extraembryonic tissue, while highlighting the cell-types that exhibited consistent upregulation and/or loss of hnRNPL as outliers.

3. DISCUSSION

Previous work has demonstrated the significance of hnRNPL as a regulator of splicing in a variety of tissues. The reported preimplantation embryonic lethality that occurs in hnRNPL-deficient mice suggests an equally vital contribution to embryonic and placental development. A careful review of newly released early lethal phenotype data produced by the Mager Lab (https://blogs.umass.edu/jmager/) confirmed that several genes identified by others as hnRNPL RNA binding targets (e.g., ATP2B1) (Fei et al., 2017) are essential for developmental progression in the mouse. Furthermore, this analysis revealed a consensus gene expression pattern in trophectoderm and extraembryonic ectoderm lineages, implicating a potential role of hnRNPL in driving differentiation or morphogenesis of these early tissues. Despite this, the mechanism by which lethality occurs remains largely unknown. For this reason, we therefore undertook a detailed spatial and temporal characterization of the expression patterns of hnRNPL in the embryo and placenta, which will provide a useful basis for further investigation of the mechanisms of hnRNPL-regulated pathways that impact normal development. This study identified: 1) presence of hnRNPL at all stages of embryonic and placental development; 2) specific upregulation of hnRNPL

in highly metabolically active tissue and cell types, specifically in the embryonic heart; 3) a unique hnRNPL expression pattern in trophoblast giant cells; 4) spatiotemporal hnRNPL regulation in mature human and mouse placenta. Taken together these findings support that hnRNPL control of embryonic and placental development occurs through cell type-specific expression.

3.1 hnRNPL is Present at All Stages of Development

Our RNA and protein analysis demonstrated sustained hnRNPL expression in the mouse embryo and placenta, from the blastocyst stage throughout the implantation period and further into placental development (Figures 1A and 5B). These results are consistent with previous work showing hnRNPL expression in undifferentiated embryonic stem cells (M. Li et al., 2015). Although a peak of hnRNPL expression was observed at the E8.5 chorion (the point of chorioallantoic fusion, which forms the intricate vasculature between the mother and fetus (Rossant & Cross, 2001), other RBPs display a similar increase, suggesting that coordinated alternative splicing may be required at E8.5. The presence of hnRNPL in both the ICM and surrounding trophectoderm cell lineages at the blastocyst stage further indicated an early functional requirement for this SF and widespread effects in both embryonic and extraembryonic tissues (Figure 1C–F). We interpret these combined findings to support further an important role of hnRNPL throughout mouse development.

3.2 hnRNPL is Upregulated in Highly Metabolic Specialized Cell Types

At later stages of development, hnRNPL was ubiquitously expressed across nearly all cell types, however, distinct patterns of expression were seen in tissues exhibiting high energic rates. One such region, the visceral endoderm (VE), is a functionally complex extraembryonic cell layer responsible for synthesizing proteins to enable nutrient uptake and delivery, while also influencing the differentiation and organization of blood vessels to facilitate in maternal-fetal exchange (Bielinska et al., 2002). Similarly, the ectoplacental cone is a structure that forms early in development and serves as a precursor to the junctional zone and invasive secondary TGCs that first contact maternal arteries (Woods et al., 2018). The relative upregulation of hnRNPL in these cells as compared to the surrounding tissue, suggests a role for this SF in in the regulation of embryonic vascularization and metabolic demands.

Notably, marked elevation of hnRNPL was seen in the uNK cells surrounding the implantation site, particularly around E7.5 (Figure 2E–G). This was an interesting finding since, in addition to the VE and EPC, uNK cells are also heavily involved in vascularization, specifically in remodeling of spiral arteries into high-capacitance, low-resistance blood vessels during pregnancy to accommodate for the nutritional demands and increased vascular load throughout development (Sojka et al., 2019). This role is reinforced by the frequent localization of uNK cells near trophoblast-lined blood vessels and murine studies showing defects in spiral remodeling in uNK deficient mice (Sojka et al., 2019). Furthermore, Gamliel et al. proposed that uNK cell function in vascular remodeling during a first pregnancy could provide a retained response recalled in subsequent pregnancies to more efficiently promote proper placental vascular development, implying even long-term functions of these cells in developmental vasculature (Gamliel et al., 2018).

The interaction of uNK cell receptors with trophoblast MHC class I proteins has been proposed to be an important controller of implantation (Moffett-King, 2002), and sufficient inhibition of uNK cells associated with specific HLA profiles contributes to the development of preeclampsia (Hiby et al., 2004). Unregulated inflammation and hypoxia are two posited pathologies for preeclampsia, and they are also triggers for the previously identified stress response pathway linking hnRNPL to disinhibition of vascular endothelial growth factor-A (*VEGFA*) mRNA (Jafarifar et al., 2011; Shih & Claffey, 1999; Venkata Subbaiah et al., 2019; Yao et al., 2013), an extensively studied proangiogenic factor whose isoforms are involved in a majority of angiogenic pathways *in vivo* (Gacche & Meshram, 2014). VEGFA disruption is also connected to a preeclampsia phenotype (Tsatsaris et al., 2003). The upregulation of hnRNPL in uNK cells could be ascribed to its function in promoting normoxic conditions and proper vascular adaptation to prevent preeclampsia. This hypothesis is supported by previously established work which has demonstrated the significance of splicing factors in the onset of preeclampsia. Multiple studies have shown that alternative splicing of the endothelial receptor Flt1 results in the production of sFlt1 splice variants that are upregulated in preeclampsia, particularly sFLT_v1 (Heydarian et al., 2009), and Flt1 splicing was further implicated in the development of fetuses reported small for gestational age (Jebbink et al., 2011). Thus, preeclampsia represents a paradigmatic example of developmental pathophysiology that correlates with splicing dysfunction.

Trophoblast giant cells are another key cell type differentiating early on from the trophectoderm layer (Rossant & Cross, 2001). Included in their many functions is the invasion of the uterine epithelium and release of hormones in later gestation, to recruit pathways for maternal adaptation (Hu & Cross, 2009). Our data revealed that TGCs displayed a particularly unique hnRNPL expression pattern at E6.5, flocalized primarily in the periphery of the nucleus rather than the usual diffuse nuclear signal (Figure 2D, 3). This novel subcellular localization may offer insight into the function of hnRNPL in these cells. The previous model of hnRNPL in hypoxic response pathways demonstrated that the re-localization of hnRNPL from the nucleus to the cytoplasm under conditions of hypoxia is essential for exerting its effect on VEGFA (Yao et al., 2013). These distinct nuclear distribution patterns specifically have also been implicated in directing chromatin dynamics and genome organization (Buchwalter et al., 2019), thus exerting influence on processes involving development, disease, and aging.

Previous studies have shown that subcellular localization of hnRNPL varies across cell types. Our novel TGC results indicate a skewed nuclear localization of hnRNPL and support that hnRNPL levels are highest on the periphery of TGC nuclei (Figure 4). This peripheral region corresponds to compartment B, a nuclear compartment from which specialized epigenetic activity is directed (Buchwalter et al., 2019). Specifically, compartment B has been shown to regulate gene positioning and chromatin organization of the genome within the nucleus, as well as gene expression levels at all levels of transcription, through the presence of nuclear pore complexes (NPCs) and laminas. As compartment B has now also been shown to exhibit unusually high levels of hnRNPL levels, there is a possibility that hnRNPL interacts with NPCs and laminas to cause these epigenetic effects during development. As discussed before, hnRNPL has been shown to have direct epigenetic effects through its relationship with SETD2 and H3K36me (Yuan et al., 2009). Thus, our TGC

localization data, in light of previously published molecular developmental epigenetics data, further supports that hnRNPL may regulate epigenetic activity in TGCs. We note as well that the relative fraction of hnRNPL within the nucleus and cytoplasmic compartments may differ throughout cell-type, development, and in postnatal aging. While this study did not investigate these potential important changes, they are the focus of ongoing investigations in our laboratory.

hnRNPL expression showed distinct patterns in the developing embryo and placenta. At E8.5, hnRNPL was most expressed in cardiac cells of the developing heart, a finding that continues to align with evidence of hnRNPL function in highly metabolic tissue types (Figure 2J–K). In support of this, our immunoblots detected highest hnRNPL protein expression in the embryonic heart, compared with postnatal. These observations is indicative of the role of this protein not only in placentation but in embryogenesis and early cardiac development. Although this was a novel finding for hnRNPL, RBPs generally have been implicated in promoting normal cardiac function, often adapting to conditions of heart failure by reverting to fetal-like activation and expression patterns (Gao et al., 2016). Interestingly, the VE is also linked to cardiomyogenesis *in vivo* and acceleration of stem cell differentiation into cardiomyocytes *in vivo* (Nijmeijer et al., 2009). This connection relates to our observations of simultaneous heightened hnRNPL levels in the VE and cardiac cells relative to the surrounding tissue. hnRNPL function in the developing heart might be in part mediated by its established interaction with Apela, which can act as a non-coding RNA (M. Li et al., 2015). Apela is highly expressed in early embryogenesis and is essential to cardiogenesis and angiogenesis. These established links relating splicing factors and the VE to cardiac function, in conjunction with the data we present here, provide an avenue for further exploration of the role of hnRNPL in the developing heart.

The expression profile of hnRNPL in the mature mouse and human placenta provides further support a specific function in specialized metabolic processes. In the E17.5 fully developed mouse placenta, hnRNPL expression appeared highest in the junctional zone (JZ), which exists between the maternal decidua and labyrinth (Figure 6). As highlighted earlier, the JZ derives from the ectoplacental cone, which also exhibited high expression of hnRNPL in earlier stages of development. The continued observation of increased expression from EPC to JZ indicates a continued use of hnRNPL in these cells throughout the period of placental development. A key feature of the JZ is the prevalence of glycogen cells present, which are believed to act as an energy reserve to provide additional nutrition to the developing placenta and embryo (Woods et al., 2018). In conjunction with the previous findings of hnRNPL expression, this raises the question whether common aspects of glucose utilization could be regulated by hnRNPL across various cell types. Of note, the glucose transporter 1 Glut1 transcript is an established target of hnRNPL (Hamilton et al., 1999). In further support of this, we observed a close association of hnRNPL expression with the cytotrophoblast layer in first trimester human placenta tissue and trophoblast lines Htr8 and Jeg3 (Figure 7G–I). Recent work has discovered the vital metabolic role of the cytotrophoblast layer of placental villi, providing evidence that it exhibits higher glycolytic rates and lactate production than the overlying syncytiotrophoblast. Mitochondrial expression and activity were enhanced in cytotrophoblasts as well, and differentiation to the merged syncytiotrophoblast layer resulted in fragmented mitochondria, indicating metabolic suppression (Kolahi et al., 2017).

Although some hnRNPL expression was seen in the overlying syncytiotrophoblast, it is likely due to recent merging of the cytrotrophoblast as they developed to form the syncytiotrophoblast.

3.3 hnRNPL-Deficient Cell Type Correlates with ER Stress Pathways

The protective effects of PRL coupled with the role of hnRNPL in PRL gene regulation provides further evidence for contributions of hnRNPL to development. Two cell types were notably hnRNPL-deficient. These include fetal red blood cells in the placenta (Fig. 2I) and decidual cells at specific stages of implantation. At E5.5 we observed the same near ubiquitous expression of hnRNPL throughout most fetal and maternal tissue, however the region directly adjacent to the developing embryo showed markedly weaker expression compared to cells further away from the implantation site (Figure 1G). Decidua is a uterine tissue that is essential for maintaining a healthy environment for embryonic development during pregnancy through various functions including hormone secretion. Prolactin (PRL) genes are among these secreted factors that have been shown to play vital roles in pregnancy, a subset of which is specifically associated with the maternal adaptations to ER stress induced by implantation and fetal growth (Alam et al., 2015). These PRL-cytokines act to dampen this stress response thus preventing harmful effects of overreactive inflammatory processes on pregnancy (Alam et al., 2015). Previous work has shown that hnRNPL influences alternative splicing and RNA stability of PRL superfamily genes (Lei et al., 2018). Therefore, the lack of hnRNPL expression that we observed in decidual cells of the implantation site may be permissive, supporting activation of ER stress programs that support implantation.

The results of this study provided qualitative evidence of hnRNPL expression throughout critical stages of development in the mouse, and support follow up investigations of hnRNPL-regulated mRNA splicing in both embryonic and placental development. Upregulation of hnRNPL in the VE, JZ, uNK cells, fetal heart, and cytotrophoblasts may correlate with critical function of hnRNPL in these highly metabolically active tissues. Given the continuously dynamic nature of the developing placenta and embryo, this also explains the ubiquity of hnRNPL in most cell types and stages. Many of these cell-types are involved with vascular remodeling and maintenance of normoxic conditions. Thus, an argument could be made for the involvement of hnRNPL in these functions as well. The time frame for the critical requirement is less clear, given the consistent expression of hnRNPL from the blastocyst stage through placental maturity. However, our observations do not contradict the previously reported preimplantation embryonic lethality that occurs with loss of hnRNPL.

Our findings on hnRNPL may have broader implications for development and human diseases. Splicing factors have been previously implicated in a variety of developmental pathways, signifying their importance during these critical stages. Furthermore, loss of, or defects in, splice variants are associated with the pathophysiology of placental disease states, which are often defined by a wide profile of altered gene expression (Ruano et al., 2021). Identifying the splicing factors and corresponding alternative mRNA isoforms that

are associated with normal and pathogenic pregnancy may aid in providing novel candidates for diagnostic markers and therapeutic targets for research.

3.4 Conclusion

In summary, we have produced a detailed analysis of hnRNPL expression and localization in the placenta and embryo throughout development. We provide multiple lines of evidence of the continued function of hnRNPL from the blastocyst stage to full placental development, as well as its involvement in multiple cell lineages. Although ubiquitous expression of hnRNPL is observed, several distinct cell types displayed notable upregulation of hnRNPL, particularly those with increased metabolic demands and involved in energic processes. These studies suggest a role for hnRNPL in early cardiac development, providing evidence for its function in both embryonic and placental development. Our data also supports a potential role for hnRNPLin TGC epigenetics through the significant peripheral nuclear localization of hnRNPL, as well as uNK cells which are critical for placental vascular remodeling and can influence preeclampsia phenotypes. Further work is needed to delineate more clearly the cell types and developmental stages that critically require hnRNPL expression and to identify specific biochemical pathways to which it contributes.

4. EXPERIMENTAL PROCEDURES

4.1 Human Placenta Analysis & Nonhuman Subjects Research (NHSR)

De-identified first trimester human placental samples were obtained from the O'Tierney-Ginn lab Human Placental Database (IRB # STUDY00000869). Placental specimens GA 11–12 weeks were collected at time of elective termination of pregnancies with informed consent.

4.2 Animal Research

This study was carried out in strict accordance with the recommendations in the Guide for the Care and Use of Laboratory Animals of the National Institutes of Health. The protocol was reviewed and approved by the Tufts Medical Center IACUC, Boston, MA, US (Protocol #2017–145). C57Bl6/j mice were purchased from the Jackson Laboratories (000664). C57Bl6/j mice were mated and developmental timing was determined by the presence of a vaginal plug the morning after mating with noon designated as E0.5. Placenta and extraembryonic tissues were collected and flash frozen or fixed as described below. Posterior embryonic trunk and tail were taken for genotyping.

4.3 Gene Expression

Embryo and placenta tissue were isolated and stored at −80°C. Total RNA was extracted using the RNeasy Mini Kit (Qiagen 74104) and DNaseI (Qiagen 1023460). cDNA synthesis was performed with 1000ng RNA. Omniscript RT Kit (Qiagen 205113) was used with both random hexamers (Qiagen 79236) according to the manufacturer's instructions. Primers used to evaluate hnRNPL mRNA expression are listed below. Gene mRNA expression was normalized to expression levels of the housekeeping gene GAPDH. hnRNPL RNA-sequencing data was obtained from BioStudies accession E-MTAB-6798 and presented as

counts per million (CPM) obtained after trimmed median of M-values normalization (TMM) in edgeR using methods from Robinson et al (Robinson et al., 2010).

Name	Sequence	Tm
hnRNPL ID 3F	CTTGGGACTACACGAACCCC	60
hnRNPL ID 3R	CCGCTTCACTCCCAGTTCAT	60
hnRNPL ID 7F	GGGCCTGATTGACGGAGTAG	60
hnRNPL ID 7R	GGGTCACCTTGTCCACTGAG	60
hnRNPL ID 7bF	CTACGCTGCAGACAACCAGA	62
hnRNPL ID 7bR	AGGGTCACCTTGTCCACTGA	44
hnRNPL ID 10F	ACCTCAGTGGACAAGGTGA	58
hnRNPL ID 10R	CCGCTTCACTCCCAGTTCAT	60

4.4 Proteomic Analyses

The Wallingford Lab Developmental Mouse Proteome Database (DMPD) (Kashpur et al, article in process) was examined to determine protein abundance levels of hnRNPL. The DMPD includes 50 independent mouse placenta proteomes produced through tandem mass spectrometry (Lumos). Three independent placenta samples isolated from three independent litters were analyzed for each developmental stage spanning E8.5 to E17.5. Between E8.5-E12.5 samples were collected every 12h and between E13.5-E17.5 sampled were collected every 24h. Low abundance proteins (>2 peptides) were filtered.

4.5 Immunofluorescence

4.5.1 Whole Mount Blastocyst Immunofluorescence—Blastocysts were collected by flushing uteri with PBS at embryonic day 3.5. Embryos were fixed for 1 hour using 4% paraformaldehyde immediately after collection on ice, permeabilized using 1% Triton X-100 and then washed prior to incubation with primary antibodies at 1:200 overnight. After washing, one hour incubation with secondary antibodies and then DAPI nuclear stain, embryos were individually transferred into single wells of chambered coverslip-slides (Ibidi) for imaging in a Nikon C2 confocal microscope. The images were taken at 20X objective. The following antibodies and antibody concentrations were used: Anti-hnRNP-L Mouse monoclonal antibody (sigma aldrich R4903 and recombinant); Anti-CDX2 antibody (1:200), Rabbit monoclonal (Abcam ab76541); alexa fluor 488 donkey anti-mouse (1:500); alexa fluor 594 donkey anti-rabbit (1:500).

4.5.2 Section Immunofluorescence—Specimens were dissected and fixed in 4% paraformaldehyde (PFA)/PBS overnight at 4°C. They were then dehydrated through a series of ethanol washes, treated with xylenes, embedded in paraffin, and sectioned at 7.5 micrometers with a Leica RM2135. Immunofluorescence was performed with a 4% normal donkey serum block and heat mediated antigen retrieval with 0.01M Tris Base pH10.0. The following antibodies and antibody concentrations were used: mouse monoclonal clone 4D11 anti-hnRNPL (Sigma-Aldrich R4903 1:200); anti-CK7 (Abcam ab181598 1:10,000); anti-E-Cadherin (CDH1) 2μg/mL (Abcam ab53033); phalloidin (PHDH1), donkey anti-

rabbit Dylight 549 7.5μg/mL (Jackson ImmunoResearch 711-505-152); donkey anti-goat Dylight 7.5μg/mL (Jackson ImmunoResearch 488 705-485-147); donkey anti-mouse Alexa Fluor 488 7.5μg/mL (Jackson ImmunoResearch 715-545-151) and donkey anti-rabbit IgG 15μg/mL (Jackson ImmunoResearch, 711-545-152). Immunofluorescence was followed by DAPI dilactate for nuclear counterstain (Life Technologies, D3571) and mounted with ProLong Gold Antifade Media (Life Technologies, P36930). Imaging was performed on a T9 Fluorescence Microscope and Calibri and ZEN 2 Pro software.

Multiple published reports have used the 4D11 anti-hnRNPL monoclonal antibody to conduct IHC, ICC, Western Blot and immunoprecipitation analyses, as well as proximity ligation assay (PLA) (Hahm et al., 1998; X. Liu & Mertz, 1995; Rossbach et al., 2009; Shih & Claffey, 1999). The antibody was validated in knockout/knockdown studies *in vivo* (Xiao Liu et al., 2020) and *in vitro*. Both nuclear and cytoplasmic localizations of hnRNPL were reported using the 4D11 clone (Coppin et al., 2017).

4.6 Semiquantitative Analysis of Protein Abundance

Images were analyzed in FIJI. hnRNPL signal in blastocysts and hnRNPL signal in E6.5 TGCs were analyzed through quantitative methods. To test whether hnRNPL is higher in trophectoderm versus inner cell mass blastocyst cells, the freehand selection tool was used to select individual nuclei on the blue-channel slices (DAPI) as regions of interest (ROIs). The selected regions were added to the ROI manager and applied to the red (anti-CDX2) and green (hnRNPL) color channels. The measurements in FIJI were set to area, mean gray value, minimum gray value, and mode gray value. The intensity level of hnRNPL in the ROIs was measured, and a student's t-test was performed to determine whether hnRNPL level was higher in trophectoderm versus TE.

Immunofluorescent hnRNPL signal was also analyzed in the nuclear center and periphery of postimplantation TGC nuclei (N=17). A size threshold of 350 um^2 was implemented to select for TGCs. The freehand selection tool was used to define regions of interest (ROI) which were then added to the ROI manager. The segmented line selection tool was used to draw a line to define and measure the long axis of the TGCs. The freehand selection tool was used to define the nuclear center at a radial distance of 20% of the length across the long axis as shown in Figure 4. The images were split into color channels and the ROIs selecting the nuclear periphery and center were utilized to assess abundance of the hnRNPL signal. The intensity of the hnRNPL signal was measured in TGCs nuclei through the raw integrated density measurement. A student's t-test was performed to determine whether hnRNPL level was greater in the nuclear center or nuclear periphery.

4.9 Immunoblotting.

Heart tissue was isolated from embryonic mice at day E9 and from neonatal mice at postnatal day 1. LV tissue was isolated from adult mice (age 22 weeks). Tissue lysates were prepared as described (Calamaras et al., 2019). Briefly, cardiac tissue was crushed on dry ice and lysed in TLB supplemented with 1mm PMSF and protease inhibitors (MilliporeSigma, 539134). After clearing the lysates by centrifugation, the protein content was quantified by BCA, and then diluted in 2x Laemmli sample buffer containing SDS

(MilliporeSigma, S-3401). Equal amounts of protein from the base of the LV were separated by SDS-PAGE, followed by transfer to nitrocellulose membrane. After blocking in 5% milk/TBST primary antibody to hnRNP-L (Sigma R4903) or to GAPDH in 5% BSA/TBST was applied. Secondary antibody was sheep anti-mouse. Membranes were visualized using the Protein-Simple FluorChem E system and images were quantified using Alpha Innotech Imager software.

Densitometry was performed using ImageJ software as described (Calamaras et al., 2019). hnRNP L band density was measured and normalized to GAPDH. Values are expressed as arbitrary densitometric units.

4.10 Statistical Analysis of Experimental Data

At least 3 independent samples per genotype were analyzed for all experimental data. The following statistical tests were used to analyze quantitative data. For comparison of two groups a p-value was determined by a two-tailed Student's T-test with unequal variance.

Supplementary Material

Refer to Web version on PubMed Central for supplementary material.

ACKNOWEDGMENTS

The Wallingford Lab is supported by NIH K99/R00HD090198 (M. Wallingford), AHA 19CDA34660038 (M. Wallingford), the Forbes Family, the Susan Saltonstall Foundation, and the Herbert J. Levine Foundation. Research contributions from the O'Tierney-Ginn Lab were supported in part by NIH R01HD091054 (P. O'Tierney-Ginn). The Blanton Lab is supported by NIH R01HL162919 (R. Blanton). Finally, the authors thank Donald H. Lunn (Falmouth, MA) for constructive discussion.

REFERENCES

Alam SMK, Konno T, & Soares MJ (2015). IDENTIFICATION OF TARGET GENES FOR A PROLACTIN FAMILY PARALOG IN MOUSE DECIDUA. Reproduction (Cambridge, England), 149(6), 625. 10.1530/REP-15-0107 [PubMed: 25926690]

Alexander MS, Hightower RM, Reid AL, Bennett AH, Iyer L, Slonim DK, Saha M, Kawahara G, Kunkel LM, Kopin AS, Gupta VA, Kang PB, & Draper I (2021). hnRNP L is essential for myogenic differentiation and modulates myotonic dystrophy pathologies. Muscle & Nerve. 10.1002/mus.27216

Bielinska M, Narita N, & Wilson DB (2002). Distinct roles for visceral endoderm during embryonic mouse development. International Journal of Developmental Biology, 43(3), 183–205. 10.1387/IJDB.10410899

Buchwalter A, Kaneshiro JM, & Hetzer MW (2019). Coaching from the sidelines: the nuclear periphery in genome regulation. Nature Reviews Genetics, 20(1), 39–50. 10.1038/s41576-018-0063-5

Calamaras TD, Baumgartner RA, Aronovitz MJ, McLaughlin AL, Tam K, Richards DA, Cooper CW, Li N, Baur WE, Qiao X, Wang G-R, Davis RJ, Kapur NK, Karas RH, & Blanton RM (2019). Mixed lineage kinase-3 prevents cardiac dysfunction and structural remodeling with pressure overload. American Journal of Physiology: Heart and Circulatory Physiology, 316(1),H145–H159. 10.1152/ajpheart.00029.2018 [PubMed: 30362822]

Cardoso-Moreira M, Halbert J, Valloton D, Velten B, Chen C, Shao Y, Liechti A, Ascenção K, Rummel C, Ovchinnikova S, Mazin PV, Xenarios I, Harshman K, Mort M, Cooper DN, Sandi C, Soares MJ, Ferreira PG, Afonso S, … Kaessmann H (2019). Gene expression

across mammalian organ development. Nature, 571(7766), 505–509. 10.1038/S41586-019-1338-5 [PubMed: 31243369]

Coppin L, Vincent A, Frénois F, Duchêne B, Lahdaoui F, Stechly L, Renaud F, Villenet C, Van Seuningen I, Leteurtre E, Dion J, Grandjean C, Poirier F, Figeac M, Delacour D, Porchet N, & Pigny P (2017). Galectin-3 is a non-classic RNA binding protein that stabilizes the mucin MUC4 mRNA in the cytoplasm of cancer cells. Scientific Reports, 7(1), 43927. 10.1038/srep43927 [PubMed: 28262838]

de Boer BA, van den Berg G, de Boer PAJ, Moorman AFM, & Ruijter JM (2012). Growth of the developing mouse heart: an interactive qualitative and quantitative 3D atlas. Developmental Biology, 368(2), 203–213. 10.1016/J.YDBIO.2012.05.001 [PubMed: 22617458]

Draper I, Tabaka ME, Jackson FR, Salomon RN, & Kopin A (2009). The evolutionarily conserved RNA binding protein SMOOTH is essential for maintaining normal muscle function. Fly, 3(4), 235–246. 10.4161/fly.9517 [PubMed: 19755840]

Fei T, Chen Y, Xiao T, Li W, Cato L, Zhang P, Cotter MB, Bowden M, Lis RT, Zhao SG, Wu Q, Feng FY, Loda M, He HH, Liu XS, & Brown M (2017). Genome-wide CRISPR screen identifies HNRNPL as a prostate cancer dependency regulating RNA splicing. Proceedings of the National Academy of Sciences, 201617467. 10.1073/pnas.1617467114

Gacche RN, & Meshram RJ (2014). Angiogenic factors as potential drug target: Efficacy and limitations of anti-angiogenic therapy. Biochimica et Biophysica Acta (BBA) - Reviews on Cancer, 1846(1), 161–179. 10.1016/J.BBCAN.2014.05.002 [PubMed: 24836679]

Gamliel M, Goldman-Wohl D, Isaacson B, Gur C, Stein N, Yamin R, Berger M, Grunewald M, Keshet E, Rais Y, Bornstein C, David E, Jelinski A, Eisenberg I, Greenfield C, Ben-David A, Imbar T, Gilad R, Haimov-Kochman R, … Mandelboim O (2018). Trained Memory of Human Uterine NK Cells Enhances Their Function in Subsequent Pregnancies. Immunity, 48(5), 951–962.e5. 10.1016/J.IMMUNI.2018.03.030 [PubMed: 29768178]

Gao C, Ren S, Lee J-H, Qiu J, Chapski DJ, Rau CD, Zhou Y, Abdellatif M, Nakano A, Vondriska TM, Xiao X, Fu X-D, Chen J-N, & Wang Y (2016). RBFox1-mediated RNA splicing regulates cardiac hypertrophy and heart failure. The Journal of Clinical Investigation, 126(1), 195. 10.1172/JCI84015 [PubMed: 26619120]

Gaudreau M-C, Grapton D, Helness A, Vadnais C, Fraszczak J, Shooshtarizadeh P, Wilhelm B, Robert F, Heyd F, & Möröy T (2016). Heterogeneous Nuclear Ribonucleoprotein L is required for the survival and functional integrity of murine hematopoietic stem cells. Scientific Reports, 6(1), 27379. 10.1038/srep27379 [PubMed: 27271479]

Gaudreau M-C, Heyd F, Bastien R, Wilhelm B, & Möröy T (2012). Alternative splicing controlled by heterogeneous nuclear ribonucleoprotein L regulates development, proliferation, and migration of thymic pre-T cells. Journal of Immunology (Baltimore, Md. : 1950), 188(11), 5377–5388. 10.4049/JIMMUNOL.1103142 [PubMed: 22523384]

Geuens T, Bouhy D, & Timmerman V (2016). The hnRNP family: insights into their role in health and disease. Human Genetics 2016 135:8, 135(8), 851–867. 10.1007/S00439-016-1683-5 [PubMed: 27215579]

Guang S, Felthauser AM, & Mertz JE (2005). Binding of hnRNP L to the Pre-mRNA Processing Enhancer of the Herpes Simplex Virus Thymidine Kinase Gene Enhances both Polyadenylation and Nucleocytoplasmic Export of Intronless mRNAs. Molecular and Cellular Biology, 25(15), 6303. 10.1128/MCB.25.15.6303-6313.2005 [PubMed: 16024770]

Hahm B, Kim YK, Kim JH, Kim TY, & Jang SK (1998). Heterogeneous nuclear ribonucleoprotein L interacts with the 3' border of the internal ribosomal entry site of hepatitis C virus. Journal of Virology, 72(11), 8782–8788. 10.1128/JVI.72.11.8782-8788.1998 [PubMed: 9765422]

Hamilton BJ, Nichols RC, Tsukamoto H, Boado RJ, Pardridge WM, & Rigby WFC (1999). hnRNP A2 and hnRNP L Bind the 3′UTR of Glucose Transporter 1 mRNA and Exist as a Complex in Vivo. Biochemical and Biophysical Research Communications, 261(3), 646–651. 10.1006/bbrc.1999.1040 [PubMed: 10441480]

Heydarian M, McCaffrey T, Florea L, Yang Z, Ross MM, Zhou W, & Maynard SE (2009). Novel Splice Variants of sFlt1 are Upregulated in Preeclampsia. Placenta, 30(3), 250–255. 10.1016/J.PLACENTA.2008.12.010 [PubMed: 19147226]

Hiby SE, Walker JJ, O'Shaughnessy KM, Redman CWG, Carrington M, Trowsdale J, & Moffett A (2004). Combinations of Maternal KIR and Fetal HLA-C Genes Influence the Risk of Preeclampsia and Reproductive Success. Journal of Experimental Medicine, 200(8), 957–965. 10.1084/JEM.20041214 [PubMed: 15477349]

Hu D, & Cross JC (2009). Development and function of trophoblast giant cells in the rodent placenta. International Journal of Developmental Biology, 54(2–3), 341–354. 10.1387/IJDB.082768DH

Hui J, Hung L-H, Heiner M, Schreiner S, Neumüller N, Reither G, Haas SA, & Bindereif A (2005). Intronic CA-repeat and CA-rich elements: a new class of regulators of mammalian alternative splicing. The EMBO Journal, 24(11), 1988–1998. 10.1038/sj.emboj.7600677 [PubMed: 15889141]

Hung LH, Heiner M, Hui J, Schreiner S, Benes V, & Bindereif A (2008). Diverse roles of hnRNP L in mammalian mRNA processing: a combined microarray and RNAi analysis. RNA (New York, N.Y.), 14(2), 284–296. 10.1261/RNA.725208 [PubMed: 18073345]

Jafarifar F, Yao P, Eswarappa SM, & Fox PL (2011). Repression of VEGFA by CA-rich element-binding microRNAs is modulated by hnRNP L. The EMBO Journal, 30(7), 1324–1334. 10.1038/emboj.2011.38 [PubMed: 21343907]

Jebbink J, Keijser R, Veenboer G, Post J. van der, Ris-Stalpers C, & Afink G (2011). Expression of Placental FLT1 Transcript Variants Relates to Both Gestational Hypertensive Disease and Fetal Growth. Hypertension, 58(1), 70–76. 10.1161/HYPERTENSIONAHA.110.164079 [PubMed: 21518965]

Koibuchi N, & Chin MT (2007). CHF1/Hey2 plays a pivotal role in left ventricular maturation through suppression of ectopic atrial gene expression. Circulation Research, 100(6), 850–855. 10.1161/01.RES.0000261693.13269.bf [PubMed: 17332425]

Kolahi KS, Valent AM, & Thornburg KL (2017). Cytotrophoblast, Not Syncytiotrophoblast, Dominates Glycolysis and Oxidative Phosphorylation in Human Term Placenta. Scientific Reports 2017 7:1, 7(1), 1–12. 10.1038/srep42941 [PubMed: 28127051]

Lei L, Cao W, Liu L, Das U, Wu Y, Liu G, Sohail M, Chen Y, & Xie J (2018). Multilevel Differential Control of Hormone Gene Expression Programs by hnRNP L and LL in Pituitary Cells. Molecular and Cellular Biology, 38(12). 10.1128/MCB.00651-17

Li J, Chen Y, Tiwari M, Bansal V, & Sen GL (2021). Regulation of integrin and extracellular matrix genes by HNRNPL is necessary for epidermal renewal. PLOS Biology, 19(9), e3001378. 10.1371/journal.pbio.3001378 [PubMed: 34543262]

Li M, Gou H, Tripathi BK, Huang J, Jiang S, Dubois W, Waybright T, Lei M, Shi J, Zhou M, & Huang J (2015). An Apela RNA-Containing Negative Feedback Loop Regulates p53-Mediated Apoptosis in Embryonic Stem Cells. Cell Stem Cell, 16(6), 669. 10.1016/J.STEM.2015.04.002 [PubMed: 25936916]

Liu X, & Mertz JE (1995). HnRNP L binds a cis-acting RNA sequence element that enables intron-dependent gene expression. Genes & Development, 9(14), 1766–1780. 10.1101/GAD.9.14.1766 [PubMed: 7542615]

Liu Xiao, Xie F, Lai G, & Wang J (2020). Roles of heterogeneous nuclear ribonucleoprotein L in enamel organ development and the differentiation of ameloblasts. Archives of Oral Biology, 120, 104933. 10.1016/j.archoralbio.2020.104933 [PubMed: 33137652]

Majumder M, Yaman I, Gaccioli F, Zeenko VV, Wang C, Caprara MG, Venema RC, Komar AA, Snider MD, & Hatzoglou M (2009). The hnRNA-binding proteins hnRNP L and PTB are required for efficient translation of the Cat-1 arginine/lysine transporter mRNA during amino acid starvation. Molecular and Cellular Biology, 29(10), 2899–2912. 10.1128/MCB.01774-08 [PubMed: 19273590]

Marcho C, Cui W, & Mager J (2015). Epigenetic Dynamics During Preimplantation Development. Reproduction (Cambridge, England), 150(3), R109. 10.1530/REP-15-0180 [PubMed: 26031750]

Moffett-King A (2002). Natural killer cells and pregnancy. Nature Reviews Immunology 2002 2:9, 2(9), 656–663. 10.1038/nri886

Nijmeijer RM, Leeuwis JW, DeLisio A, Mummery CL, & Chuva de Sousa Lopes SM (2009). Visceral endoderm induces specification of cardiomyocytes in mice. Stem Cell Research, 3(2–3), 170–178. 10.1016/J.SCR.2009.06.003 [PubMed: 19631601]

Robinson MD, McCarthy DJ, & Smyth GK (2010). edgeR: a Bioconductor package for differential expression analysis of digital gene expression data. Bioinformatics (Oxford, England), 26(1), 139–140. 10.1093/BIOINFORMATICS/BTP616 [PubMed: 19910308]

Rossant J, & Cross JC (2001). Placental development: Lessons from mouse mutants. Nature Reviews Genetics 2001 2:7, 2(7), 538–548. 10.1038/35080570

Rossbach O, Hung L-H, Schreiner S, Grishina I, Heiner M, Hui J, & Bindereif A (2009). Auto- and cross-regulation of the hnRNP L proteins by alternative splicing. Molecular and Cellular Biology, 29(6), 1442–1451. 10.1128/MCB.01689-08 [PubMed: 19124611]

Ruano CSM, Apicella C, Jacques S, Gascoin G, Gaspar C, Miralles F, Méhats C, & Vaiman D (2021). Alternative splicing in normal and pathological human placentas is correlated to genetic variants. Human Genetics 2021 140:5, 140(5), 827–848. 10.1007/S00439-020-02248-X [PubMed: 33433680]

Sarkans U, Gostev M, Athar A, Behrangi E, Melnichuk O, Ali A, Minguet J, Rada JC, Snow C, Tikhonov A, Brazma A, & McEntyre J (2018). The BioStudies database-one stop shop for all data supporting a life sciences study. Nucleic Acids Research, 46(D1), D1266–D1270. 10.1093/NAR/GKX965 [PubMed: 29069414]

Shih S-C, & Claffey KP (1999). Regulation of Human Vascular Endothelial Growth Factor mRNA Stability in Hypoxia by Heterogeneous Nuclear Ribonucleoprotein L. Journal of Biological Chemistry, 274(3), 1359–1365. 10.1074/jbc.274.3.1359 [PubMed: 9880507]

Sojka DK, Yang L, & Yokoyama WM (2019). Uterine Natural Killer Cells. Frontiers in Immunology, 0(MAY), 960. 10.3389/FIMMU.2019.00960

Tsatsaris V, Goffin F, Munaut C, Brichant J-F, Pignon M-R, Noel A, Schaaps J-P, Cabrol D, Frankenne F, & Foidart J-M (2003). Overexpression of the Soluble Vascular Endothelial Growth Factor Receptor in Preeclamptic Patients: Pathophysiological Consequences. The Journal of Clinical Endocrinology & Metabolism, 88(11), 5555–5563. 10.1210/JC.2003-030528 [PubMed: 14602804]

Venkata Subbaiah KC, Wu J, Potdar A, & Yao P (2019). hnRNP L-mediated RNA switches function as a hypoxia-induced translational regulon. Biochemical and Biophysical Research Communications, 516(3), 753–759. 10.1016/j.bbrc.2019.06.106 [PubMed: 31255281]

Wallingford MC, Angelo JR, & Mager J (2013). Morphogenetic analysis of peri-implantation development. Developmental Dynamics, 242(9), 1110–1120. 10.1002/dvdy.23991 [PubMed: 23728800]

Woods L, Perez-Garcia V, & Hemberger M (2018). Regulation of Placental Development and Its Impact on Fetal Growth—New Insights From Mouse Models. Frontiers in Endocrinology, 9, 570. 10.3389/fendo.2018.00570 [PubMed: 30319550]

Yao P, Potdar AA, Ray PS, Eswarappa SM, Flagg AC, Willard B, & Fox PL (2013). The HILDA Complex Coordinates a Conditional Switch in the 3′-Untranslated Region of the VEGFA mRNA. PLOS Biology, 11(8), e1001635. 10.1371/JOURNAL.PBIO.1001635 [PubMed: 23976881]

Yuan W, Xie J, Long C, Erdjument-Bromage H, Ding X, Zheng Y, Tempst P, Chen S, Zhu B, & Reinberg D (2009). Heterogeneous Nuclear Ribonucleoprotein L Is a Subunit of Human KMT3a/Set2 Complex Required for H3 Lys-36 Trimethylation Activity in Vivo. Journal of Biological Chemistry, 284(23), 15701–15707. 10.1074/jbc.M808431200 [PubMed: 19332550]

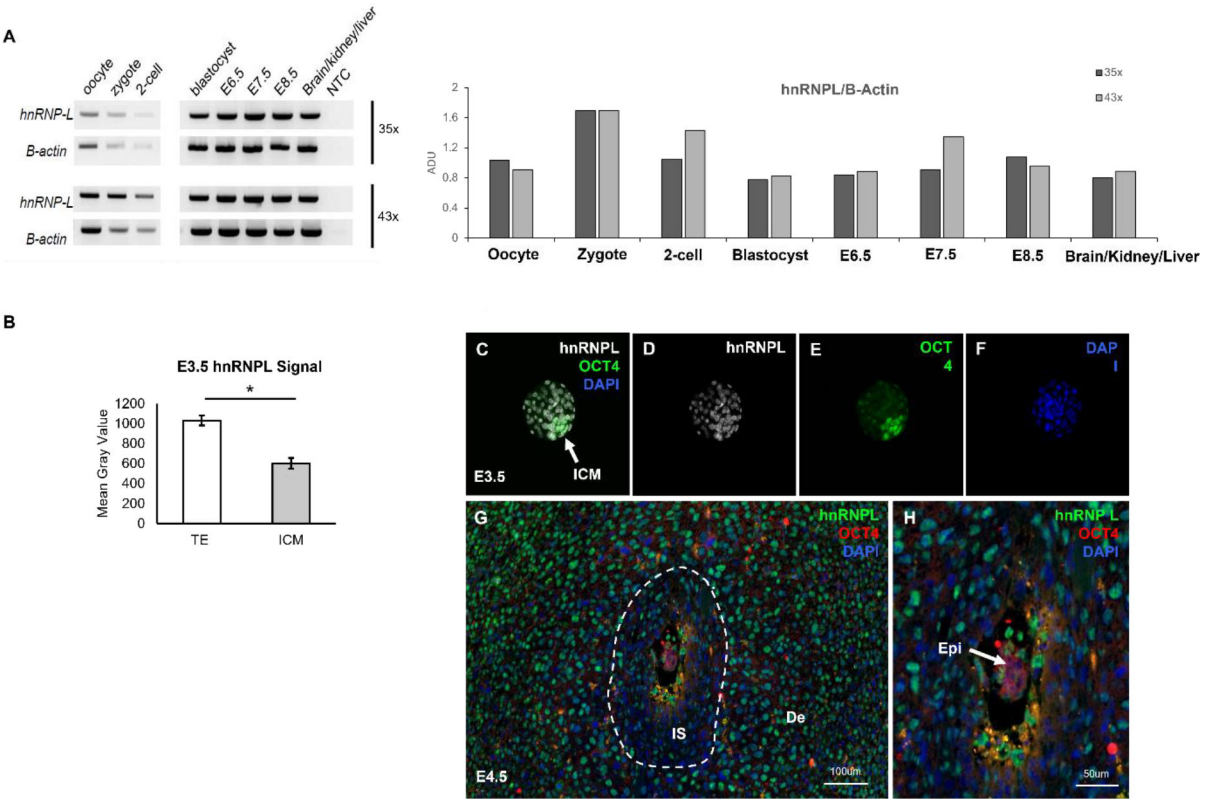

Figure 1. Preimplantation and Peri-implantation hnRNPL Expression.

(A) RT-PCR detected expression of hnRNPL mRNA in the mouse oocyte and embryo between 2-cell and E8.5 developmental stages. mRNA levels detected after 35x PCR cycles. Quantitation by densitometry is shown to the right. (B-F) Protein localization and semi-quantitative analysis of hnRNPL in the trophectoderm and inner cell mass at the E3.5 blastocyst stage (N=7 blastocysts). (B) Semiquantitative image analysis of hnRNPL stained blastocysts reflected a significantly higher level in TE as compared to ICM (p-value=1.55319E-05). (C-F) Nuclear hnRNPL (white) was observed in OCT4 (green) positive inner cell mass cells and OCT4 negative trophectoderm in the blastocyst by whole mount IHC. (G,H) Following implantation, tissue section IHC of hnRNPL (green) and OCT4 (red) reveals cell type-specific patterns at the implantation site at E4.5. *Abbreviations:* De, decidua; Epi, epiblast; ICM, inner cell mass; IS: implantation site.

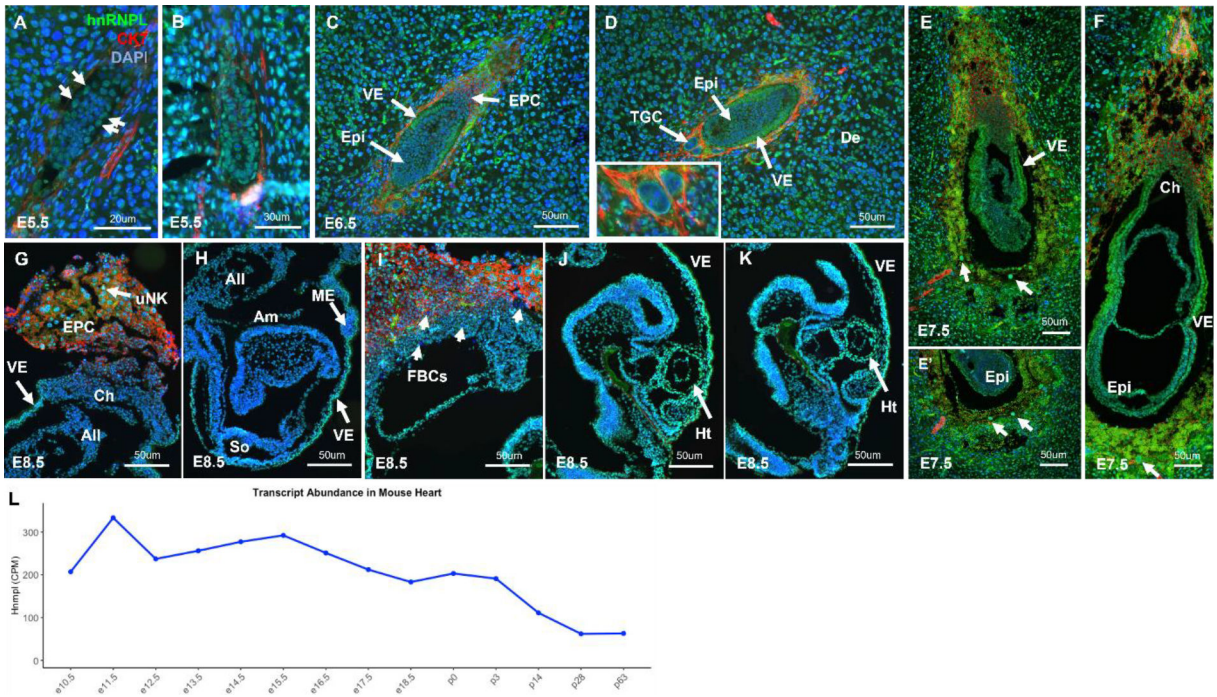

Figure 2. Peri-implantation and Gastrulation hnRNPL Expression.

Following implantation, tissue section IF of hnRNPL (green) and CK7 (red) reveals cell type-specific patterns between E5.5 and E8.5. (A-D) Abundant hnRNPL can be differentiated in the extraembryonic visceral endoderm between E5.5 and E6.5. Arrows are shown to denote the various cell types present in the developing embryo, including the visceral endoderm, ectoplacental cone, and epiblast layer, as well as the surrounding maternal decidua (A-D). (D) Trophoblast giant cells surrounding the implantation site exhibit unique expression patterns of hnRNPL in the nuclear periphery. (E-K) Strong hnRNPL signal is retained in the VE through E7.5 and E8.5 in the embryo proper as well as in isolated cells pointed out with arrows at the periphery of the implantation site, likely corresponding to uterine natural killer cells (E-K). (I) Fetal blood cells were observed in the placenta and yolk sac that were strikingly negative or low in hnRNPL protein (arrows). (J-K) Within the embryo proper, fetal cardiac tissue displayed differentially increased hnRNPL protein levels that rivalled the level observed in the extraembryonic VE (arrows). (L) VE and uNK cells retained high hnRNPL signal through E8.5. Developmental expression of hnRNPL in heart was determined from RNA-sequencing data from wild-type CD-1 mice (Cardoso-Moreira et al., 2019; Sarkans et al., 2018). Presented as counts per million (CPM) obtained after trimmed median of M-values normalization (TMM) in edgeR using methods from (Robinson et al., 2010) *Abbreviations:* All, allantois; Am, amnion; C, chorion; Dec, decidua; EPC, ectoplacental cone; Epi, epiblast; FBC, fetal blood cells; Ht, heart; ME, mesoderm of the yolk sac; uNK, uterine natural killer cell; VE, visceral endoderm; TGC, trophoblast giant cell.

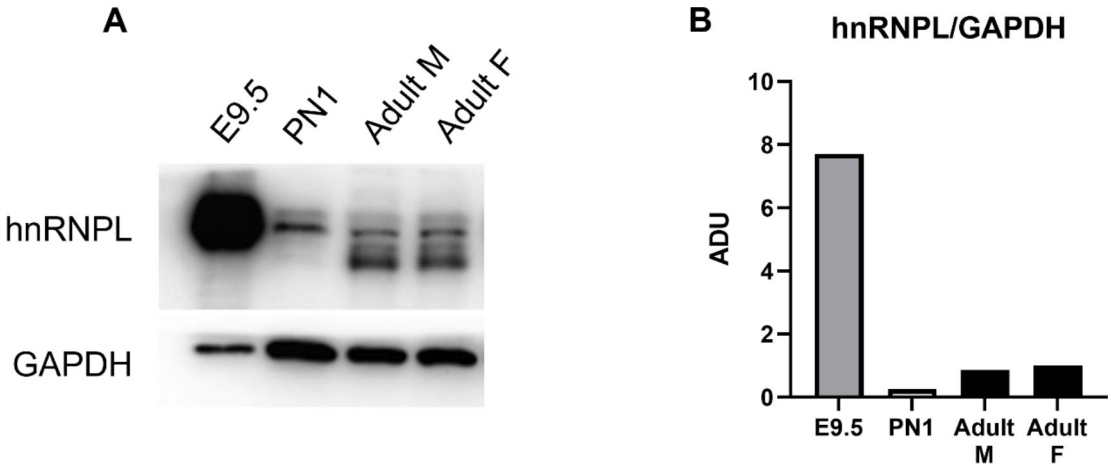

Figure 3. hnRNPL expression in embryonic, neonatal, and adult heart.

(A) Immunoblot of hnRNPL and GAPDH in mouse heart tissue from: embryonic day 9.5 (E9.5, pooled from one litter); neonatal postnatal day 1 (PN1); and adult male and female (22 week-old). (B) Densitometry of hnRNP normalized to GAPDH. ADU, arbitrary densitometric units.

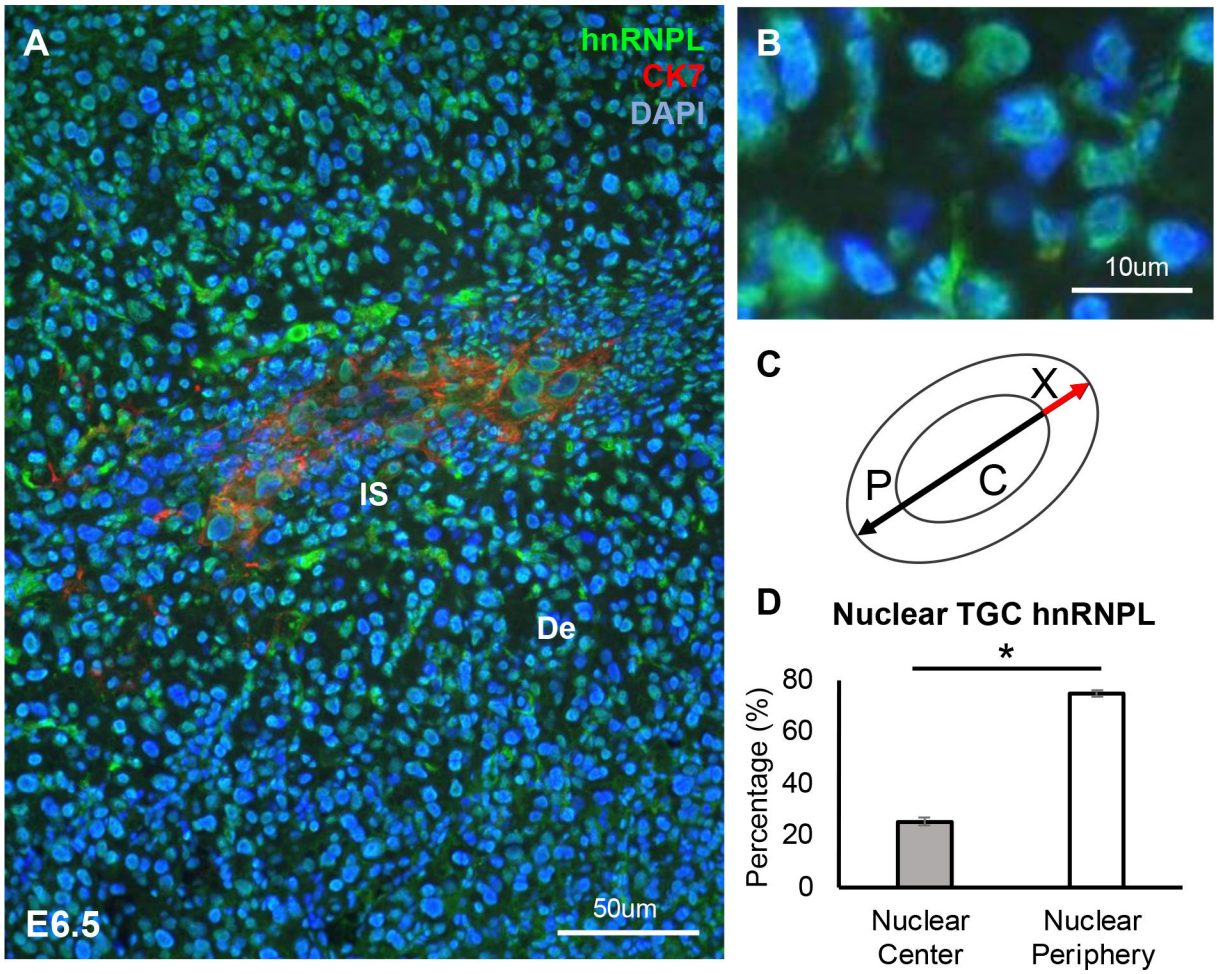

Figure 4. Trophoblast Giant Cell Nuclear hnRNPL Distribution.

(A, B) Immunofluorescent detection of hnRNPL (green) and CK7 (red) at E6.5. Observed hnRNPL protein signal displayed a potential bias towards the nuclear periphery in TGCs of the implantation site (IS). (C, D) Compartmental hnRNPL signal was analyzed in the nucleus through a semi-quantitive image analysis approach using FIJI. Signal abundance measures for the central (C) versus the peripheral (P) nuclear compartment of TGC nuclei were compared as diagrammed in C. Integrated density measurements of E6.5 TGC nuclei (N=17) revealed a significant increase in hnRNPL signal in the nuclear periphery as compared to the central compartment (p-value=4.24888E-23). *Abbreviations:* C, central compartment; De, decidua; P peripheral compartment; IS, implantation site; X, variable representing 20% of the length of the longitudinal diameter which was used to define the peripheral region of TGC nuclei.

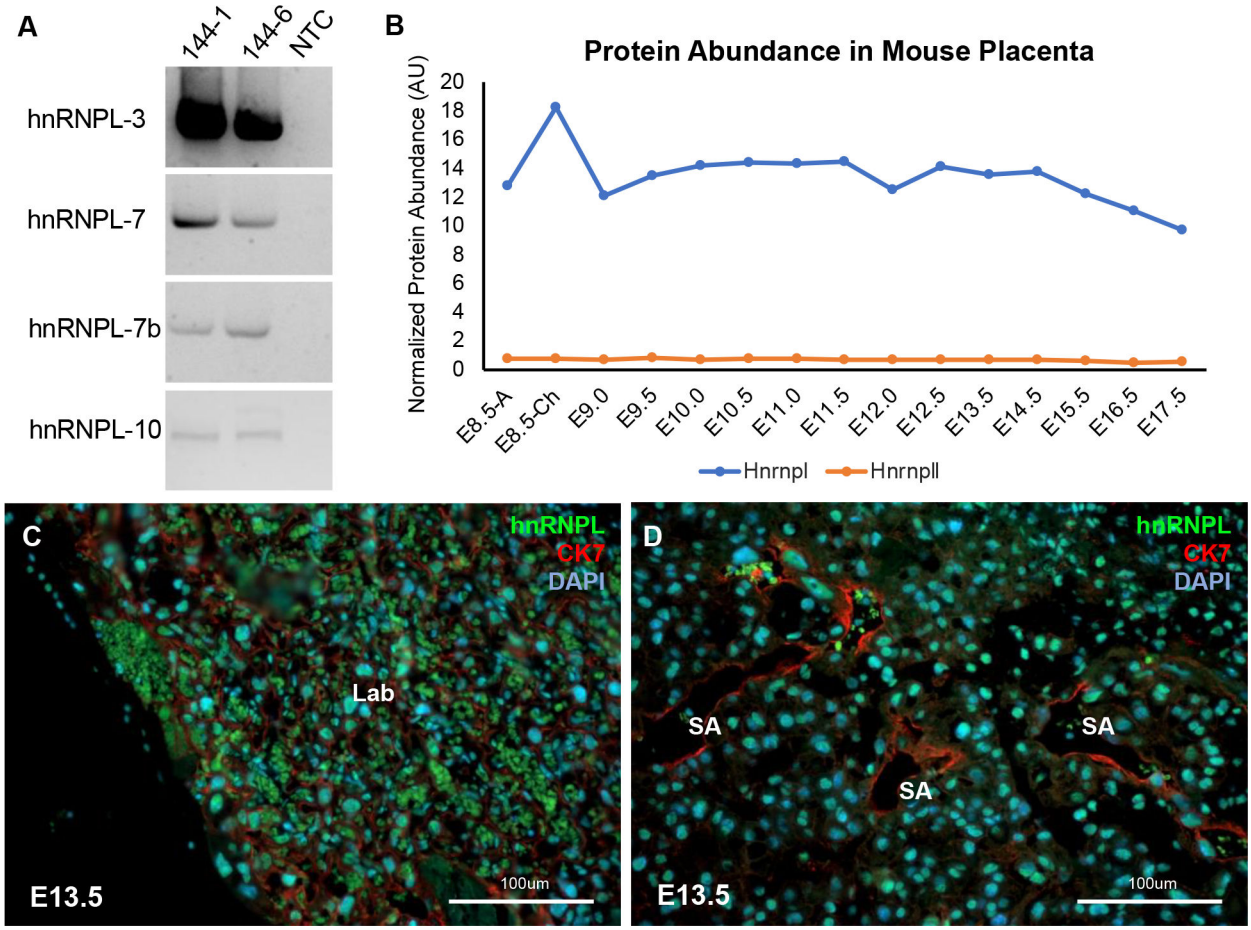

Figure 5. hnRNPL Protein in the Fully Developed Mouse Placenta.

(A) RT-PCR confirms hnRNPL mRNA in the E13.5 mouse placenta. Two independent replicates are shown (144-1 and 144-6) alongside a no template control (NTC). (B) Tandem mass spectrometry reveals steady expression of hnRNPL protein from E8.5 to E17.5, and modest peak in hnRNPL expression is observed in the chorion at E8.5. The hnRNPL paralog hnRNPLL is not detected at significant levels. (C and D) hnRNPL (green signal) is detected throughout the labyrinth of the fully developed E13.5 placenta, adjacent to trophoblasts denoted by cytokeratin 7 (red). (D) hnRNPL signal was also present in cells next to CK7-outlined spiral arteries present at this stage. *Abbreviations:* CK7, cytokeratin 7; Lab, labyrinth; SA, spiral arteries.

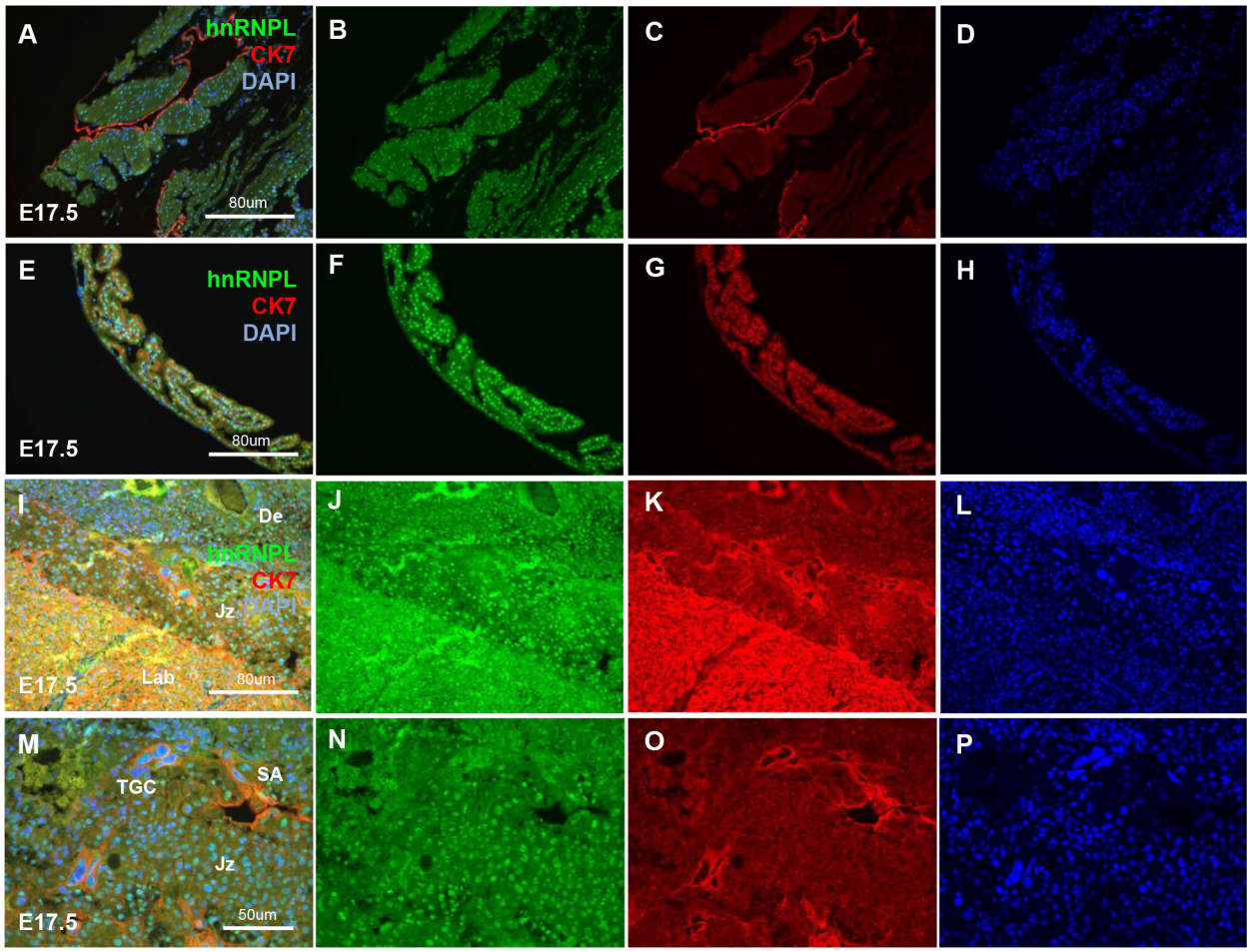

Figure 6. hnRNPL Protein in the Mature Placenta.

(A-H) Adjacent to the placenta at E17.5 hnRNPL (green) was detected in uterine muscle and in visceral endoderm of the yolk sac. (C, G) Cytokeratin 7 (red) outlined adjacent trophoblasts in these sections (C, G). (I, L) Within the placenta at E17.5 hnRNPL is detected diffusely in the decidua, junctional zone, and labyrinth. (M-P) Uniformly higher levels of hnRNPL protein are observed in the Jz, which is shown at a higher magnification. CK7 identifies trophoblasts here both in the labyrinth (K) and lining spiral arteries that punctate the Jz (O). *Abbreviations:* CK7, cytokeratin 7; De, decidua, Jz, junctional zone; Lab, labyrinth; SA, spiral artery; TGC, trophoblast giant cell.

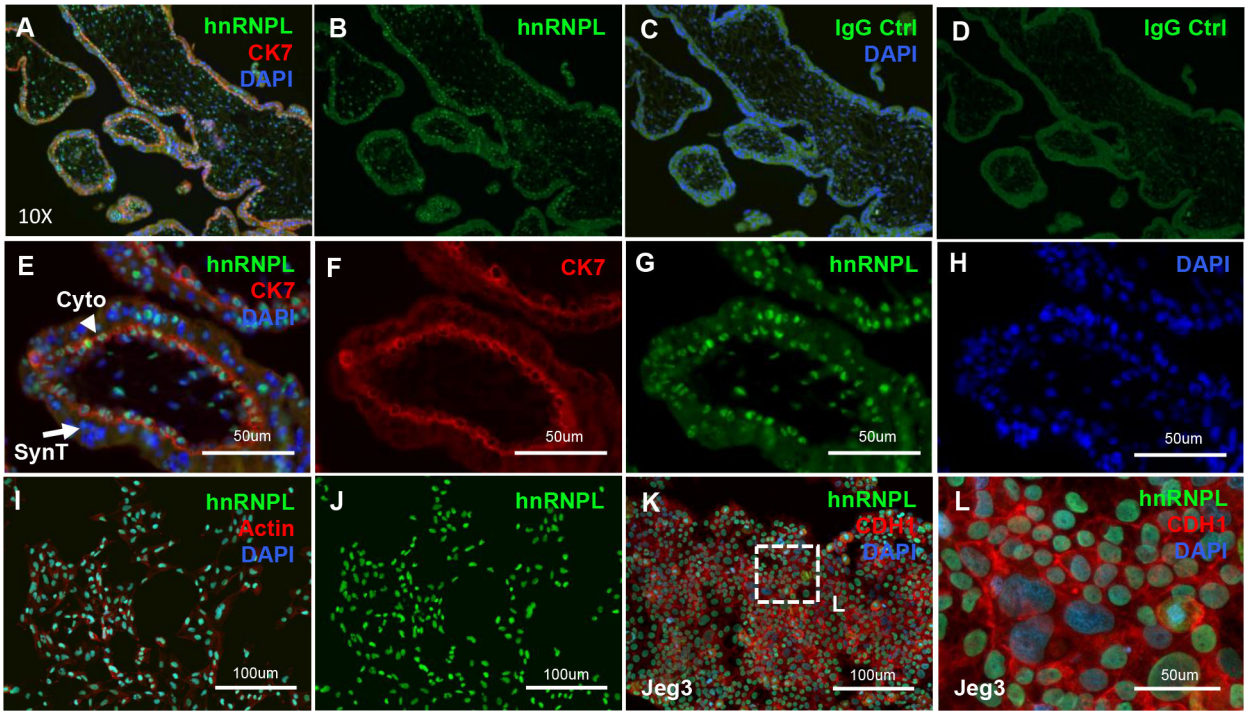

Figure 7. hnRNPL Protein in the Human Placenta and Placental Cell Lines.

(A,B) hnRNPL (green) is expressed in first trimester human placenta. (C,D) IgG isotype negative control is included for comparison. (E-H) In the first trimester human chorionic villi hnRNPL colocalizes with cytokeratin 7 (red) positive cytotrophoblasts that outline the villi lumen (arrowhead) whereas the majority of syncytiotrophobast nuclei have minimal hnRNPL (arrow). (I-J) hnRNPL was detected in trophoblast cell lines: the Htr8 cell line counterstained with phalloidin which binds actin (I-L) and Jeg3 cell line counterstained with anti-CDH1 (K,L). (L) The observed hnRNPL Jeg3 expression was not uniform and was downregulated in syncytialized Jeg3 nuclei. *Abbreviations:* CK7, cytokeratin 7; Cyto, cytotrophoblasts; SynT, syncytiotrophoblast.

Table 1.

hnRNPL Expression Summary.

hnRNPL expression was observed using immunofluorescence and evaluated based on a relative comparison of expression levels. Signal from the cells surrounding the implantation site was used as a baseline reference. Presence and relative quantification of hnRNPL expression were denoted using pluses (+) and absence of hnRNPL expression was denoted using minuses (−).

Stage/Region	hnRNPL Expression Level
Blastocyst	
Inner Cell Mass	++
Trophectoderm	+++
Post-Implantation	
Epiblast	++
Visceral Endoderm	+++
Ectoplacental Cone	+++
Trophoblasts	+++
Trophoblast Giant Cells	++
Uterine Natural Killer Cells	++++
Decidua	++
Junctional Zone	+++
Labyrinth	++
Fetal Blood Cells	-